ACS Chemical Neuroscience

Research Article

pubs.acs.org/acschemicalneuroscience

X-ray Absorption Spectroscopy at the Sulfur K-Edge: A New Tool to Investigate the Biochemical Mechanisms of Neurodegeneration

Mark J. Hackett,[†] Shari E. Smith,[‡] Phyllis G. Paterson,[‡] Helen Nichol,[§] Ingrid J. Pickering,[†] and Graham N. George*[,†]

[†]Molecular and Environmental Sciences Group, Department of Geological Sciences, University of Saskatchewan, 114 Science Place, Saskatoon, Saskatchewan S7N5E2, Canada

[‡]College of Pharmacy and Nutrition, University of Saskatchewan, 110 Science Place, Saskatoon, Saskatchewan S7N5C9, Canada

[§]Department of Anatomy and Cell Biology, University of Saskatchewan, 107 Wiggins Road, Saskatoon, Saskatchewan, S7N5E5, Canada

ABSTRACT: Sulfur containing molecules such as thiols, disulfides, sulfoxides, sulfonic acids, and sulfates may contribute to neurodegenerative processes. However, previous study in this field has been limited by the lack of in situ analytical techniques. This limitation may now be largely overcome following the development of synchrotron radiation X-ray absorption spectroscopy at the sulfur K-edge, which has been validated as a novel tool to investigate and image the speciation of sulfur in situ. In this investigation, we build the foundation required for future application of this technique to study and image the speciation of sulfur in situ within brain tissue. This study has determined the effect of sample preparation and fixation methods on the speciation of sulfur in thin sections of rat brain tissue, determined the speciation of sulfur within specific brain regions (brain stem and cerebellum), and identified sulfur specific markers of peroxidative stress following metal catalyzed reactive oxygen species production. X-ray absorption spectroscopy at the sulfur K-edge is now poised for an exciting new range of applications to study thiol redox, methionine oxidation, and the role of taurine and sulfatides during neurodegeneration.

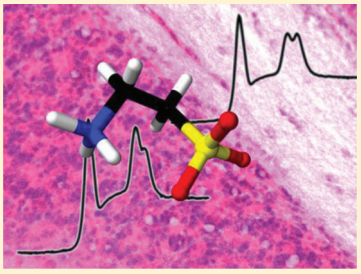

KEYWORDS: *Sulfur, cerebellum, neurodegeneration, thiol-redox, taurine, XAS*

With aging populations, the development of effective treatment(s) for neurodegenerative disease remains one of the greatest challenges to modern medicine. Elucidation of the biochemical mechanisms of disease pathogenesis is crucial to guide drug and therapy design. However, despite extensive research into neurodegeneration, abnormalities in some key chemical pathways remain unclear.

Studying the metabolomics of sulfur compounds shows strong potential to reveal new insight into the pathogenesis of neurodegeneration during cerebral ischemia (i.e., stroke),[1−12] Parkinson's disease,[13−19] Alzheimer's disease,[20−26] Friedreich's ataxia,[27] and multiple sclerosis.[28,29] Traditionally, biochemical assays of the ratio of cellular thiols to disulfides, or more specifically the reduced to oxidized glutathione ratio, have been used as markers of peroxidative stress within brain tissue.[2−4,9,10,14,16,18] However, further research in this field has been hindered by the lack of tools to show the distribution of altered sulfur redox. For example, there is no isotope of sulfur for which NMR or MRI measurements are practical. Likewise, immunohistochemical methods have encountered significant problems, with inconsistent tissue penetration of labeling antibodies and stains resulting in conflicting results.[15,30] Two photon fluorescence imaging of glutathione shows potential, however this method requires a suitable fluorescence tag with uniform tissue and cell penetration.[31] Analysis of microdissected tissue regions, or cellular and subcellular fractions of tissue homogenates with enzymatic assays, fluorescence assays or separation techniques (i.e., chromatography) coupled to mass spectroscopy can in part compensate for the lack of more direct methods.[32,33] These techniques quantify specific sulfur molecules, but the methods cannot be performed in situ. Due to the sensitive nature of sulfur-containing molecules, redox alterations during sample preparation can confound results with these approaches.[2,3,9,10,32,33] Other techniques with strong potential to study (image) the sulfur metabolome in situ are mass spectral imaging (MSI) methods, such as time-of-flight secondary ion mass spectrometry (TOF-SIMS) and matrix-assisted laser desorption ionization mass spectrometry (MALDI-MS). While analysis of hydrated sections is often problematic, these methods have been applied to freeze-dried tissue sections, at a spatial resolution of 50−100 μm.[34−37]

In addition to sulfur redox, other sulfur containing molecules, such as taurine and sulfatides, play critical roles in several signaling pathways during neurodegeneration.[1,5−7,25] Therefore, the study of the sulfur metabolome and the role of specific sulfur species in addition to sulfur redox, during neurodegeneration, is of significant interest.

Received: October 7, 2011
Accepted: January 2, 2011
Published: January 2, 2012

Table 1. Effect of Sample Preparation on the Speciation of Sulfur within Thin Sections of Rat Cerebellum (percentage contribution of sulfur functional groups)[a]

method	disulfide	thiol[b]	thio-ether[b]	sulfoxide	sulfinic acid	sulfonic acid	sulfate ester
frozen unfixed hydrated	2.6(6) ± 1.0	54(2) ± 4	25(2) ± 3	1.0(3) ± 0.6	1.1(4) ± 0.5	11.2(3) ± 1.5	4.4(2) ± 3.3
air-dried (60 s)	4.3(3) ± 0.9[c]	56(1) ± 18	23(1) ± 22	2.7(1) ± 0.1[d]	nd[e]	9.6(1) ± 1.8	4.1(1) ± 1.6
air-dried (1 week)	5.6(4) ± 1.9[c]	50(1) ± 5	27(1) ± 2	2.6(2) ± 0.9[c]	nd[e]	9.5(2) ± 0.18	5.4(1) ± 1.4
freeze dried	4.7(5) ± 0.9[c]	50(1) ± 5	28(1) ± 3	2.2(1) ± 0.3[c]	nd[e]	9.0(2) ± 1.0	6.2(1) ± 1.8
formaldehyde fixed	14.3(5) ± 3.7[d]	44(1) ± 14	31(2) ± 16	4.1(2) ± 0.4[e]	nd[e]	nd[e]	6.2(1) ± 5.1

[a]Values given are the average percentages ± standard deviation of triplicate measurements; the values in parentheses are the average estimated standard deviation from the individual fits (given as the last digit of the percentage) obtained from the diagonal elements of the covariance matrices and assuming a constant variance across the range of individual spectra. The estimated standard deviation gives an indication of how well each component is determined, whereas the standard deviation of the triplicate measurements gives an indication of how much variation is present between different samples. We note that, as expected for slightly different individual fits, the average percentages do not total to 100%, although the individual fits do total to 100%. A value of 0% was assigned for components that could not be detected (nd). [b]The thiol and thio-ether components possess similar spectra that are slightly displaced in energy and hence exhibit a high mutual correlation in the fit, which is reflected in the higher values for the estimated standard deviation. [c]A significant difference in average percent composition values between frozen unfixed hydrated tissue and tissues prepared with other methods was determined with the Student's *t* test and a 95% confidence limit: *p*-value <0.05. [d]*p*-value < 0.01. [e]*p*-value <0.001.

In this study, we show how X-ray absorption spectroscopy (XAS) at the sulfur K-edge (~2469 eV) can be used to directly investigate the speciation of sulfur and determine alterations in sulfur redox, in situ, in brain tissue. Due to the large energy range over which the K-edge of specific electronic states of sulfur absorb (14 eV), this method is ideally suited to discriminate between sulfur species of differing electronic structure (i.e., disulfides, thiols, thio-ethers, sulfoxides, sulfinic acids, sulfonic acids, and sulfates). Previous work using synchrotron radiation as the incident X-ray source has yielded high quality data within a short time period (several minutes) for organic (coal) and biological samples (bacteria, blood, plasma, erythrocytes, and onion tissue).[38−43] Specifically, two studies have already demonstrated the significant potential of the method to study sulfur redox in situ within biological samples.[41,43] In addition, the method has recently been applied to study neuromelanin within formalin-fixed paraffin embedded brain tissue and isolated and purified human neuromelanin.[44,45]

This study extends from these previous reports, and investigates sulfur speciation in specific regions of the rat brain and how tissue fixation and peroxidatvie stress induced in vitro may change these species. The goal is to build a solid technical platform for future studies using XAS at the sulfur K-edge to image and examine the role of sulfur-containing molecules in the brain during neurodegenerative disease.

RESULTS AND DISCUSSION

Data Fitting and Elucidation of Sulfur Speciation. It has been established that the near edge spectrum collected from a sample comprised of multiple contributing chemical components can be successfully fitted to a linear sum of the individual spectra collected from each pure component.[38,41] Previously, this method has been used to determine the speciation of sulfur in coals, bacteria, onion tissue, blood, and mammalian cell samples.[38−43] In this study, model compounds that reflect the range of sulfur functional groups known to be present in brain tissue at concentrations of 10 μM or greater were chosen as initial standards for fitting (Table 1). Using this approach, sulfur K-edge spectra of brain tissue were fitted to a linear combination of the pure spectra of compounds representative of disulfides, thiols, thio-ethers, sulfoxides, sulfinic acids, sulfonic acids, and sulfates (sulfate esters and inorganic sulfate) (Figures 1 and 2). Inorganic sulfate was removed from the fits, as it was not found to contribute significantly. The relative concentrations of these compounds present in the rat cerebellum, determined from the fitting procedure are presented in Table 1. Due to the closeness of the fits and low residuals obtained from the fitting method, it is concluded that no other functional groups at levels detectable by XAS are present. In all cases, the fit residuals were a value of 0.5 or less, which is less than values previously reported in the literature.[40]

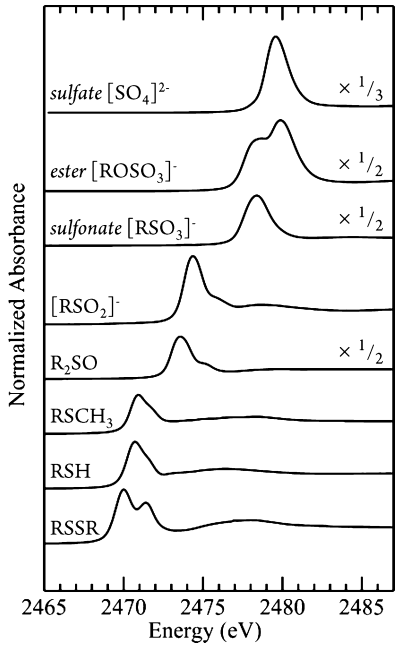

Figure 1. Sulfur K-edge X-ray absorption spectra of representative sulfur species in aqueous solution at pH 7.4 (except for sulfate and ester, pH 8.2). All spectra were normalized to the height of the edge-jump after background removal. Spectra were vertically scaled as indicated for clarity.

Effects of Sample Preparation. The sensitivity of sulfur to redox chemistry is well established, and may be responsible for many conflicting results within the literature.[2,3,9,10,46,47] Therefore, sample preparation methods for in situ analyses of tissue sections post mortem must be judiciously selected to ensure the results reflect the original tissue composition prior to death.

dx.doi.org/10.1021/cn200097s | ACS Chem. Neurosci. 2012, 3, 178−185

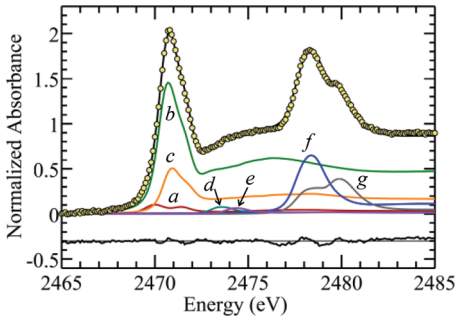

Figure 2. Representative analysis of a sulfur K-edge spectrum collected from a 10 μm thick section of frozen unfixed hydrated rat cerebellum tissue to a linear combination of standard spectra. The normalized experimental data are shown as points, with the results from the least-squares fit shown as the black line. The reference spectra of pure components, scaled to their relative contribution to the fit are also shown: *a*, disulfide; *b*, thiol; *c*, thio-ether; *d*, sulfoxide; *e*, sulfinic acid; *f*, sulfonate; and *g*, sulfate ester. The vertically displaced lower trace shows the residual.

Traditional methods in histology incorporate fixation and paraffin embedding to preserve tissue morphology. Although highly successful, an often overlooked fact is that these methods best retain the morphology of relatively large tissue components (i.e., proteins, organelles, and whole cells). It has been demonstrated that significant leaching of smaller, hydrophilic molecules and diffusible ions, as well as oxidation of tissue components occur during fixation procedures.[48] In this investigation, the relative speciation of sulfur (disulfide, thiol, thio-ether, sulfoxide, sulfinic acid, sulfonic acid, and sulfate) was determined for frozen unfixed hydrated, formaldehyde-fixed, unfixed air-dried (air-dried for 60 s and 1 week), and unfixed freeze-dried rat cerebellum tissue sections (Table 1).

The results reveal that formaldehyde-fixed tissue contains the lowest content of sulfonic acids, compared to sections prepared by other methods (Table 1). Taurine, a small hydrophilic molecule, is the most abundant sulfonic acid within the cerebellum, present in millimolar concentrations.[25,34,36,49−53] Therefore, the reduced sulfonic acid content within formaldehyde-fixed tissue is attributed to leaching of taurine during immersion in the aqueous formaldehyde solution (see Figure 3A). In agreement with this conclusion, no difference in sulfonic acid content was observed between the other preparation methods, which did not involve immersion of the tissue in an aqueous medium. In addition to a reduced relative content of sulfonic acids, there was a reduction in the total sulfur content of formalin-fixed tissue, further emphasizing the effect of fixation induced leaching (data not shown).

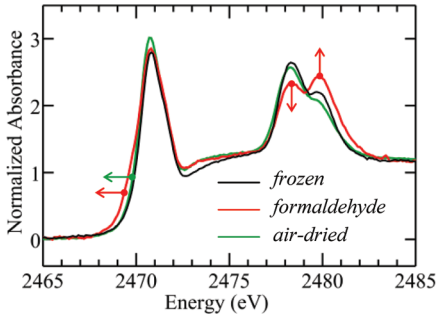

Figure 3. Representative spectra showing the effect of sample preparation on the sulfur near-edge spectra. Spectra from frozen unfixed hydrated sections (black) and formaldehyde-fixed sections (red) are compared with air-dried sections (green). Arrows emphasize differences between the spectra.

In contrast with the reduction in sulfonic acid content, formaldehyde-fixed tissue contained the highest relative concentration of disulfides and sulfoxides (Table 1). As both disulfides and sulfoxides are well-known products of thiol and thio-ether peroxidation,[46,47] this result strongly supports the occurrence of tissue peroxidation during fixation. The most likely source of the peroxidative damage is the aqueous fixation medium which may mediate the production and propagation of free radicals, as previously suggested.[48] While these results highlight the susceptibility of tissues to fixation induced leaching and peroxidation artifacts, it must be noted that the fixation procedure used in this study was performed on thin tissue sections, rather than bulk tissue. It is possible that the lipid rich exterior of a whole intact brain acts as a hydrophobic barrier, minimizing the leaching effects that occur during fixation of the whole brain compared to thin sections.

Similar to formaldehyde-fixed tissue a significant increase in the relative disulfide content (see Table 1) was observed in partially and completely air-dried (60 s and 1 week, respectively) and freeze-dried tissue (relative to frozen hydrated tissue). The broadening and shift in the position of the multicomponent (disulfides, thiols, thio-ethers) edge at ∼2470 eV as a consequence of the increase in disulfides is presented in Figure 3). However, no difference in disulfide content was observed between sections air-dried for 60 s or one week. This result suggests that tissue peroxidation is mediated by free radicals generated within the aqueous medium of hydrated tissue, and therefore, ceases upon dehydration. As such, thawing of the tissue sections was identified as the sample preparation step most likely to introduce peroxidation artifacts in nonformaldehyde-fixed tissues. With this in mind, one would expect freeze-dried tissue sections, where water is removed via sublimation from the frozen state, to display significantly less peroxidation artifacts than air-dried sections. This hypothesis was not supported by the results. However, it must be noted that during transfer of tissue sections from the cryostat to the freeze-dryer, the sections came into brief contact (several seconds) with air at room temperature. It is believed that this would have resulted in partial thawing of the tissue surface, which could account for the relative increase in disulfide content of freeze-dried tissue. Therefore, a modified freeze-dryer setup that prevents tissue thawing during transfer could potentially minimize or prevent tissue peroxidation and preserve the sulfur redox status.

As shown in Table 1 and Figure 2, a sulfinic acid component was included in the fitting process for all spectra; however, a significant contribution to fits was observed only in frozen hydrated tissue. Even in this instance, the average relative contribution was 1.1%. Likewise, in the frozen hydrated tissue, disulfides and sulfoxides contributed only 2.6 and 1.0%, respectively, to the fits. Nonetheless, removal of any of these minor components from the fits resulted in an increase in the fit residuals (Figure 2).

Due to artificial oxidation the contribution of disulfides and sulfoxides was significantly larger in spectra collected from tissue prepared by the other methods. However, no contributions from sulfinic acids were detected. The major sulfinic acid expected to be present within brain tissue is hypotaurine, which occurs at concentrations of approximately

Table 2. Differences in the Speciation of Sulfur between the Rat Cerebellum and Brain Stem (percentage contribution of sulfur functional groups)[a]

tissue	disulfide	thiol	thio-ether	sulfoxide	sulfinic acid	sulfonic acid	sulfate ester
cerebellum	2.6(6) ± 1.0	54(2) ± 4	25(2) ± 3	1.0(3) ± 0.6	1.1(4) ± 0.5	11.2(3) ± 1.5	4.4(2) ± 3.3
brain stem	4.6(8) ± 3.1	64(3) ± 5*	15(3) ± 8*	1.1(2) ± 1.6	0.2(2) ± 0.2*	3.8(4) ± 1.9*	11.0(2) ± 1.3*

[a]A significant difference in mean percent composition values between frozen unfixed hydrated cerebellum and brain stem tissue was determined with the Student's *t* test and a 95% confidence limit. Values are the mean percent composition ± standard deviation of triplicate measurements. The mean esd values obtained from fitting are given in parentheses (see Table 1).

10 μM which is near the detection limit of our measurments.[54,55] Hypotaurine is a relatively reactive intermediate, which has been shown in vitro to enzymatically or spontaneously (in the presence of UV) oxidize to taurine.[54,55] As such, we propose that hypotaurine is likely to be converted to taurine upon tissue thawing and therefore, the contribution from sulfinic acids would be below detection limits in all samples except frozen hydrated tissue sections. Based on these results, we estimate a detection limit of 10 μM for these measurements.

Another source of peroxidative artifacts during our analysis are oxygen-based free radicals (e.g., hydroxyl) generated during exposure of the samples to the X-ray beam. Indeed, visual analysis of frozen hydrated tissue after data collection revealed the presence color centers from hydrated electrons trapped in the ice matrix (i.e., a pink stripe where the sample was exposed to the beam). However, only on comparison of an initial spectrum to the subsequent third or fourth spectra collected from one sample were the effects of beam damage observed. No alterations were observed between the first two spectra recorded for a sample. However, this does not exclude beam damage during collection of the first spectrum. If beam damage due to free radical production was occurring to a significant extent, it would be expected that significant differences in the levels of oxidized and reduced sulfur species would be observed between partially or completely air-dried tissue sections (due to variation in the tissue water content). No significant difference in the relative content of any of the sulfur species was observed between partially or completely air-dried tissue. This observation indicates that the results from this study are purely due to oxidative changes induced during sample preparation, and not preferential generation of radicals during data collection.

These results have revealed that the in vivo sulfur redox state of brain tissue is best preserved in frozen hydrated tissue, which also prevents leaching of water-soluble species. It is recommended that cryofixation and analysis of frozen tissue sections be adopted as the standard for this research. Although peroxidation artifacts were observed in air-dried or freeze-dried tissue sections, these methods will retain the distribution of sulfur containing molecules (i.e., no leaching artifacts). Therefore, air-dried or freeze-dried sections may be suitable for future imaging studies of higher oxidation state sulfur species such as sulfonic acids and sulfates. Moreover, an improved design on the current freeze-dryer apparatus may completely prevent thawing of the tissue sections and, therefore, better preserve the sulfur redox state.

As significant leaching and oxidation artifacts were observed in formaldehyde-fixed tissue sections, this sample preparation method is not recommended for future studies of this nature. It is acknowledged that characterization of the sulfur containing molecules that are not removed during immersion in an aqueous medium (i.e., sulfatides) may allow a limited scope for future XAS studies on formaldehyde-fixed tissue.

Effects of Tissue Thickness. The relatively low energy of X-rays at the sulfur K-edge and associated short penetration depth into biological tissue necessitates the need for thin samples. Consequently, investigation of sulfur chemistry during neurodegeneration will most likely be limited to in situ analysis of thin sections of brain tissue, or in vitro studies of single cells. One area of concern for analyses of tissue sections is ensuring that the chemical composition of the section accurately reflects the in vivo composition. During sectioning and melting of the thin section onto a suitable substrate (i.e., therminox coverslip), it is possible that artifacts may be introduced. To investigate this effect, the relative composition of sulfonic acids and sulfates in sections of brain tissue of 4, 6, 8, and 10 μm was investigated. The major sulfonic acid species present in brain tissue is taurine, a free water-soluble amino acid, whereas the major sulfate species are sulfatides, structurally bound long chain lipids. Therefore, artifacts induced in the sectioning process would be expected to manifest as an increasing or decreasing trend in the relative contribution of either or both of these species across tissue sections of increasing thickness. As expected, the relative contribution of taurine and sulfate, when multiplied by the edge jump, shows an increasing trend with greater tissue thickness (data not shown). However, no such trend is seen in the normalized spectra, indicating that any artifacts introduced during sectioning are independent of tissue thickness, giving further confidence that the sulfur speciation within unfixed frozen hydrated sections accurately reflects the in vivo state. Further, the increasing trend did not display a plateau at increasing tissue thickness, which suggests that self-absorption (a common problem for XAS at the sulfur K-edge)[41,42] was not occurring.

Discrimination between Tissue Types. Until now the speciation of sulfur within specific regions of the brain could only be studied by microdissection followed by tissue homogenization, extraction, and biochemical assay. Therefore, past studies have been limited by sample preparation artifacts that occur during these steps. In addition, the brain regions that could be studied were limited to those that could be successfully microdissected.

To investigate the ability of sulfur K-edge XAS to determine sulfur speciation within different tissue types, spectra were collected from thin sections of rat brain stem or cerebellum. The results presented in Table 2 and Figure 4 show significantly higher thiol, thio-ether, and sulfonic acid, and lower sulfate content within the cerebellum, relative to the brain stem. These differences are in direct accordance with the known cellular composition of these two brain regions. For example, myelinated axons of white matter are known to contain higher sulfate concentration (predominantly sulfatides) than neuron bodies within gray matter, which are known to contain higher concentrations sulfonic acids (predominantly

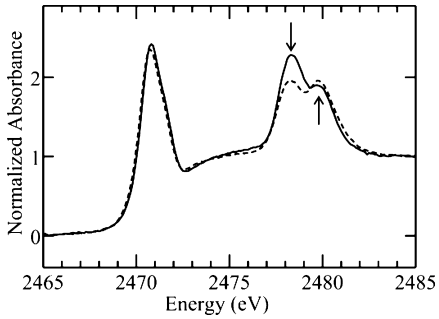

Figure 4. Representative spectra from 10 μm thick sections of cerebellum (solid line) and brain stem (broken line) showing the differences in relative abundance of taurine and sulfate esters (arrows) between these two brain regions.

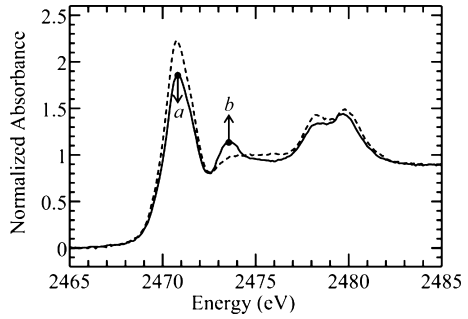

Figure 5. Effect of peroxidative stress on the speciation of sulfur. Representative spectra of tissue sections incubated in PBS (broken line) and in a solution of Fe(II) (solid line), showing the relative decrease in reduced forms (*a*, 2470.3 eV) and increase in sulfoxides (*b*, 2473.5 eV) together with more subtle changes in other forms.

taurine).[25,34,36,49−53] Due to the high content of granular neuron bodies within the cerebellum, and the sparse distribution of cell bodies in the brain stem (which is predominantly white matter), a higher sulfonic acid concentration within the cerebellum, and a higher sulfate concentration within the brain stem is expected. Moreover, it is known that thiols and thio-ethers form a large component of proteins within cell bodies, and would occur in greater concentration within the cerebellum.

Although this level of biochemical information has been previously reported,[50−52] and can be obtained from a variety of methods, this is the first study to reveal this information from a single in situ measurement. These results highlight the ability of sulfur K-edge XAS to determine sulfur speciation in situ, to differentiate between different tissue types. This demonstrates the significant potential of future microprobe and imaging experiments, which will determine the speciation of sulfur from a sample volume of <1 μm, in cryo-fixed tissue. The ability to obtain this information without the need for microdissection, homogenization, or extraction procedures is expected to reveal unprecedented detail regarding the role of sulfur- containing molecules in stroke and degenerative disorders.

Markers of Peroxidative Stress. It is well-known that conditions of peroxidative stress occur during many brain diseases or disorders, and result in an increase in the abundance of disulfides and sulfoxides within biological samples. Moreover, the reaction pathways have been characterized such that the initial conversion of thiols or thio-ethers to disulfides is often followed by conversion of disulfides to sulfoxides.[46,47] To assess the ability of XAS to detect the sulfoxide end products of excessive tissue peroxidation, sulfur speciation was determined for tissue sections subjected to transition metal catalyzed free radical production. As shown in Figure 5, a substantial increase in the level of sulfoxides (4.9% to 13.2%) but not disulfides was observed following incubation of tissue sections in Fe(II). The increase in sulfoxides in the tissue section incubated with Fe(II) was observed with a corresponding decrease in the relative composition of thiols (56.5% to 35.4%) The absence of an increase in disulfides is attributed to the severity of peroxidation induced, with disulfide products being further oxidized to sulfoxides, and/or leaching of disulfide products from the tissue sections into the aqueous incubation medium.

It is known that peroxidative stress during disease can result in the addition of sulfoxide functional groups to peptides and proteins which drastically alters their function.[46,47] In situ images of the distribution of sulfoxides within the brain may significantly increase our knowledge regarding the effects of sulfoxide addition to proteins and cell physiology. Further, due to many proposed roles for altered metal homeostasis during brain diseases, future experiments that will image the distribution of sulfoxides relative to redox active Fe and Cu are an exciting prospect to understand further the role of metals in brain function.

■ CONCLUSIONS

We note that a previous study has investigated the speciation of sulfur in situ within formalin-fixed paraffin embedded human brain tissue.[44] This previous study assumed a priori that consistent fixation and embedding protocol would not have differential effects on the speciation of sulfur for control and diseased sample groups. However, this assumption does not take into account differential binding to certain tissues of redox active metal contaminants in fixation media, redistribution and differential binding to certain tissues of endogenous redox active compounds, and the potential for differential leaching between healthy and diseased tissue.[48] Therefore, when studying the underlying biochemical mechanisms of disease, comparable effects of fixation between sample groups, even with consistent preparation protocols should not be assumed without prior investigation.

In this study, sulfur K-edge XAS has been used for the first time for semiquantitative in situ determination of cerebral disulfides, thiols, thio-ethers, sulfinic acids, sulfonic acids, and sulfates, at the relative concentrations most likely to be present in vivo. Comparison of the results obtained from several sample preparation protocol revealed a significant increase in the relative concentration of sulfur peroxidation products (disulfides and sulfoxides) upon thawing of brain tissue and/or immersion in an aqueous medium. This strongly supports the use of frozen, unfixed hydrated tissue and analysis under cryo-conditions for future work. In the absence of suitable cryogenic conditions, freeze-drying was shown to be most likely to best preserve the sulfur redox state of the tissue. For studies not concerned with sulfur redox, but purely aimed at imaging the distribution of higher oxidation state sulfur species (sulfonic acids and sulfates), air-dried sections would suffice. However, due to the leaching and peroxidation artifacts associated with formaldehyde-fixation, this sample preparation method should be avoided.

Using frozen, unfixed, hydrated tissue, differences in sulfur speciation between the brain stem and cerebellum were characterized, and the results shown to be consistent with the known composition of these two regions. To the best of our

knowledge, this is the first direct in situ investigation of the sulfur biochemistry between specific brain regions. As such, this investigation opens the door to future microprobe applications of the technique to image the distribution of sulfur containing molecules at the cellular and subcellular level. An imaging approach will be further valuable in minimizing artificial peroxidation during sample preparation. Traditionally, animal brains are perfused to remove blood which would contribute to sulfur measurements. However, the act of perfusion creates ischemic conditions within the brain, leading to peroxidative stress. Using an imaging approach, sulfur speciation can be determined for discrete brain regions of flash frozen brain tissue that does not need to be perfused, without risk of contamination from cerebral blood.

Finally, the ability to detect increases in sulfur oxidation products under conditions of peroxidative stress was demonstrated. This highlights the relevance of this technique to the field of neurochemistry, where questions concerning free-radical-mediated tissue damage, either by ischemia−reperfusion or alterations in metal homeostasis, can now be addressed.

METHODS

Preparation of Cerebellum and Brain Stem Tissue Sections. This work was approved by the University of Saskatchewan's Animal Research Ethics Board, and adhered to the Canadian Council on Animal Care guidelines for humane animal use. Healthy 11 week old male Sprague−Dawley rats (n = 3) were anaesthetised with isoflurane (100% O_2) inhalation and perfused with 0.9% NaCl solution. The brains were rapidly removed and dissected on an ice-cold dissection stage. The cerebellum and brain stem were embedded in a glycerol based optimal cutting temperature (OCT) tissue embedding medium and snap frozen in a liquid-nitrogen cooled iso-pentane slurry. As previously described, due to the polar nature of the glycerol components within the OCT, and the lipophilic exterior of the brain, little to no penetration of OCT through the tissue occurred.[48] The time from animal sacrifice to cryofixation was recorded and did not exceed 5 min for any animal.

Thin sagittal sections (10-μm-thick) of tissue (referred to as cryosections herein) were cut on a cryomicrotome, cooled to −16 °C, and mounted on sulfur-free Thermanox (Thermo Scientific) plastic coverslips. Five sets of tissue sections (frozen unfixed hydrated, formaldehyde-fixed, air-dried for 60 s, air-dried for 1 week, and freeze-dried) were prepared from the cryosections. To prepare the frozen unfixed hydrated sections, the cryosections were transported in a sealed vessel from the cryotome on dry ice and then stored for one week at −80 °C until required for analysis. To prepare formaldehyde-fixed sections the cryosections were air-dried for 60 s and then immersed in a 10% buffered formaldehyde solution (Sigma-Aldrich) for one hour at pH 7.4. Following fixation the sections were air-dried and stored above desiccant until required for analysis. Complete or partially air-dried sections were prepared from the cryosections, and were air-dried (over desiccant) either for one week (complete air-drying) or for 60 s (partial air drying) prior to analysis. Freeze-dried sections were prepared from cryosections via placement under vacuum conditions at −80 °C for 12 h. Triplicate samples were prepared for each of the above sample preparation methods.

Investigation of the Effects of Tissue Thickness. In addition to the 10-μm-thick tissue sections cut, as described above, an additional 5 replicate sections were cut at 4, 6, 8, and 10 μm thickness (20 sections total). These sections were mounted on therminox coverslips and air-dried above desiccant for 1 week prior to analysis.

Incubation of Cerebellum Tissue with Fe(II). To investigate the effects of transition metal-catalyzed peroxidation on the speciation of sulfur within brain tissue, spectra were collected from two 10-μm-thick cryosections of cerebellum, prepared as described above and incubated for one hour at room temperature in either PBS (pH 7.4) or a solution of 1 mM of Fe(II) ($FeCl_2$) in PBS (pH 7.4). The sections were air-dried for 60 s prior to analysis.

Standard Compounds. Standard compounds (Sigma-Aldrich) representative of disulfides (oxidized glutathione), thiols (reduced glutathione), thio-ethers (methionine), sulfoxides (methionine sulfoxide), sulfinic acids (hypotaurine), sulfonic acids (taurine), sulfate esters (dextran sulfate), and inorganic sulfates (Na_2SO_4) functional groups were analyzed as solutions (to minimize the artifacts previously reported),[41,42] made up to 30 −100 mM in PBS at pH 7.4 (except for dextran which was analyzed at pH 8.2). Solutions were analyzed in sulfur free polycarbonate cells with a polypropylene window (built in house).

Data Acquisition. All sulfur K-edge XAS data were collected at the Stanford Synchrotron Radiation Lightsource, using beamline 4−3, and employing a Si(111) double monochromator. The incident beam was reduced to 2 × 6 mm by vertical and horizontal slits, and intensity measured with a helium gas filled I_0 ion chamber. The approximate monochromatic beam intensity at the sample was 10^{11} photons/second. Samples (tissue sections and solutions) were mounted at 45° to the incident beam, and X-ray fluorescence collected with a Stern-Heald Lytle detector filled with nitrogen gas. Prior to spectra collection, the sample chamber was purged with He (to remove any water vapor that may condense on tissue surface) until the relative O_2 content within the chamber was less than 0.5%. X-ray absorption spectra were calibrated against the spectrum of a $Na_2S_2O_3.5H_2O$ powder solid standard, with the lowest energy peak set to 2469.2 eV, as described previously.[39−42,56] Spectra acquisition was controlled with XAS data collect software,[57] with spectra collected across the energy range 2450 − 2515 eV, with a total collection time of approximately 5 min. For frozen tissue sections a helium cryostream was used. The temperature of the therminox coverslip, as measured with a thermocouple, was approximately −40 °C. All other spectra were recorded at room temperature. Samples were transferred from an airtight sealed container on dry ice into the cryostream in less than 5 s. Evidence for ice crystal formation on the tissue surface (i.e., X-ray diffraction peaks in spectra) was only observed in tissue sections for which transfer took longer than 30 s.

Data Processing. Spectra were processed using the EXAFSPAK suite of programs.[58] Using the DATFIT program, spectra collected from tissue sections were fitted with a linear combination of reference spectra (see standard compounds). Standards were excluded from the refinements algorithm if they contributed to 0.5% of the total spectra, at a value greater than three times their standard deviation of measurement (calculated from the diagonal elements of the variance-covariance matrix). A significant difference in the composition of the individual sulfur was determined with a student's t-test and a 95% confidence limit.

AUTHOR INFORMATION

Author Contributions

All authors were involved in experimental design and planning. M.J.H., S.E.S., and P.G.P. performed animal experiments. M.J.H., I.J.P., and G.N.G. performed and interpreted the XAS data. M.J.H. and G.N.G. drafted the manuscript and all authors assisted in producing the final version.

Funding

This work was supported by a joint Canadian Institutes of Health Research (CIHR) / Heart and Stroke Foundation Synchrotron of Canada team grant; Synchrotron Medical Imaging (SMI) CIF99472, awarded to H.N., P.G.P., I.J.P., G.N.G. and others. M.J.H. is a Saskatchewan Health Research Foundation postdoctoral fellow, an SMI postdoctoral fellow and a fellow in the CIHR-Training grant in Health Research Using Synchrotron Techniques (CIHR-THRUST) Fellow (I.J.P. and others). G.N.G. and I.J.P. are Canada Research Chairs. Portions of this research were carried out at the Stanford Synchrotron Radiation Lightsource, a Directorate of

SLAC National Accelerator Laboratory and an Office of Science User Facility operated for the U.S. Department of Energy Office of Science by Stanford University. The SSRL Structural Molecular Biology Program is supported by the DOE Office of Biological and Environmental Research, and by the National Institutes of Health, National Center for Research Resources, Biomedical Technology Program (P41RR001209).

Notes

The authors declare no competing financial interest.

■ ACKNOWLEDGMENTS

We thank the SSRL staff, Angela Auriat, Elam Zeini and Roger C. Prince for their assistance with XAS data acquisition.

■ REFERENCES

(1) Albrecht, J., and Schousboe, A. (2005) Taurine Interaction with Neurotransmitter Receptors in the CNS: An Update. *Neurochem. Res. 30*, 1615−1621.

(2) Cooper, A. J. L., Pulsinelli, W. A., and Duffy, T. E. (1980) Glutathione and Ascorbate During Ischemia and Postischemic Reperfusion in Rat Brain. *J. Neurochem. 35*, 1242−1245.

(3) Folbergrová, J., Rehncrona, S., and Siesjö, B. K. (1979) Oxidized and reduced glutathione in the rat brain under normoxic and hypoxic conditions. *J. Neurochem. 32*, 1621−1627.

(4) Rehncrona, S., Folbergrova, J., Smith, D. S., and Siesjo, B. K. (1980) Influence of Complete and Pronounced Incomplete Cerebral Ischemia and Subsequent Recirculation on Cortical Concentrations of Oxidized and Reduced Glutathione in the Rat. *J. Neurochem. 34*, 477−486.

(5) Saransaari, P., and Oja, S. S. (1997) Enhanced taurine release in cell-damaging conditions in the developing and ageing mouse hippocampus. *Neuroscience 79*, 847−854.

(6) Saransaari, P., and Oja, S. S. (1998) Mechanisms of ischemia-induced taurine release in mouse hippocampal slices. *Brain Res. 807*, 118−124.

(7) Saransaari, P., and Oja, S. S. (2000) Taurine and neural cell damage. *Amino Acids 19*, 509−526.

(8) Satoh, T., and Yoshioka, Y. (2006) Contribution of reduced and oxidized glutathione to signals detected by magnetic resonance spectroscopy as indicators of local brain redox state. *Neurosci. Res. 55*, 34−39.

(9) Shivakumar, B. R., Kolluri, S. V., and Ravindranath, V. (1995) Glutathione and protein thiol homeostasis in brain during reperfusion after cerebral ischemia. *J. Pharmacol. Exp. Ther. 274*, 1167−1173.

(10) Shivakumar, B. R., Kolluri, S. V. R., and Ravindranath, V. (1992) Glutathione homeostasis in brain during reperfusion following bilateral carotid artery occlusion in the rat. *Mol. Cell. Biochem. 111*, 125−129.

(11) Bobyn, P. J., Franklin, J. L., Wall, C. M., Thornhill, J. A., Juurlink, B. H. J., and Paterson, P. G. (2002) The effects of dietary sulfur amino acid deficiency on rat brain glutathione concentration and neural damage in global hemispheric hypoxia - Ischemia. *Nutr. Neurosci. 5*, 407−416.

(12) Bobyn, P. J., Corbett, D., Saucier, D. M., Noyan-Ashraf, M. H., Juurlink, B. H. J., and Paterson, P. G. (2005) Protein-energy malnutrition impairs functional outcome in global ischemia. *Exp. Neurol. 196*, 308−315.

(13) Heales, S. J. R., Menzes, A., and Davey, G. P. (2010) Depletion of glutathione does not affect electron transport chain complex activity in brain mitochondria: Implications for Parkinson disease and postmortem studies. *Free Radical Biol. Med. 50*, 899−902.

(14) Patsoukis, N., Papapostolou, I., Zervoudakis, G., Georgiou, C. D., Matsokis, N. A., and Panagopoulos, N. T. (2005) Thiol redox state and oxidative stress in midbrain and striatum of weaver mutant mice, a genetic model of nigrostriatal dopamine deficiency. *Neurosci. Lett. 376*, 24−28.

(15) Pearce, R. K. B., Owen, A., Daniel, S., Jenner, P., and Marsden, C. D. (1997) Alterations in the distribution of glutathione in the substantia nigra in Parkinson's disease. *J. Neural Transm. 104*, 661−677.

(16) Perry, T. L., Godin, D. V., and Hansen, S. (1982) Parkinson's disease: A disorder due to nigral glutathione deficiency? *Neurosci. Lett. 33*, 305−310.

(17) Riederer, P., Sofic, E., Rausch, W.-D., Schmidt, B., Reynolds, G. P., Jellinger, K., and Youdim, M. B. H. (1989) Transition Metals, Ferritin, Glutathione, and Ascorbic Acid in Parkinsonian Brains. *J. Neurochem. 52*, 515−520.

(18) Sian, J., Dexter, D. T., Lees, A. J., Daniel, S., Agid, Y., Javoy-Agid, F., Jenner, P., and Marsden, C. D. (1994) Alterations in glutathione levels in Parkinson's disease and other neurodegenerative disorders affecting basal ganglia. *Ann. Neurol. 36*, 348−355.

(19) Zeevalk, G. D., Razmpour, R., and Bernard, L. P. (2008) Glutathione and Parkinson's disease: Is this the elephant in the room? *Biomed. Pharmacother. 62*, 236−249.

(20) Bains, J. S., and Shaw, C. A. (1997) Neurodegenerative disorders in humans: the role of glutathione in oxidative stress-mediated neuronal death. *Brain Res. Rev. 25*, 335−358.

(21) Balazs, L., and Leon, M. (1994) Evidence of an oxidative challenge in the Alzheimer's brain. *Neurochem. Res. 19*, 1131−1137.

(22) Berlett, B. S., and Stadtman, E. R. (1997) Protein oxiation in aging, disease, and oxidative stress. *J. Biol. Chem. 272*, 20313−20316.

(23) Dringen, R. (2000) Metabolism and functions of glutathione in brain. *Prog. Neurobiol. 62*, 649−671.

(24) Han, X. (2007) Potential mechanisms contributing to sulfatide depletion at the earliest clinically recognizable stage of Alzheimer's disease: a tale of shotgun lipidomics. *J. Neurochem. 103*, 171−179.

(25) Han, X., M., Holtzman, D., W., McKeel, D., Kelley, J., and Morris, J. C. (2002) Substantial sulfatide deficiency and ceramide elevation in very early Alzheimer's disease: potential role in disease pathogenesis. *J. Neurochem. 82*, 809−818.

(26) Perry, T. L., Yong, V. W., Bergeron, C., Hansen, S., and Jones, K. (1987) Amino acids, glutathione, and glutathione transferase activity in the brains of patients with Alzheimer's disease. *Ann. Neurol. 21*, 331−336.

(27) Calabrese, V., Lodi, R., Tonon, C., D'Agata, V., Sapienza, M., Scapagnini, G., Mangiameli, A., Pennisi, G., Stella, A. M. G., and Butterfield, D. A. (2005) Oxidative stress, mitochondrial dysfunction and cellular stress response in Friedreich's ataxia. *J. Neurol. Sci. 233*, 145−162.

(28) Choi, I.-Y., Lee, S.-P., Denney, D. R., and Lynch, S. G. (2010) Lower levels of glutathione in the brains of secondary progressive multiple sclerosis patients measured by ^{1}H magnetic resonance chemical shift imaging at 3 T. *Mult. Scler. 17*, 289−296.

(29) Srinivasan, R., Ratiney, H., Hammond-Rosenbluth, K. E., Pelletier, D., and Nelson, S. J. (2010) MR spectroscopic imaging of glutathione in the white and gray matter at 7 T with an application to multiple sclerosis. *Magn. Reson. Imaging 28*, 163−170.

(30) Hjelle, O. P., Chaudhry, F. A., and Ottersen, O. P. (1994) Antisera to glutathione: Characterisation and immunocytochemical application to the rat cerebellum. *Eur. J. Neurosci. 6*, 793−804.

(31) Sun, X., Shih, A. Y., Johannssen, H. C., Erb, Li, P., and Murphy, T. H. (2006) Two-photon Imaging of Glutathione Levels in Intact Brain Indicates Enhanced Redox Buffering in Developing Neurons and Cells at the Cerebrospinal Fluid and Blood-Brain Interface. *J. Biol. Chem. 281*, 17420−17431.

(32) Bean, M. F., Pallante-Morell, S. L., Dulik, D. M., and Fenselau, C. (1990) Protocol for liquid chromatography/mass spectrometry of glutathione conjugates using postcolumn solvent modification. *Anal. Chem. 62*, 121−124.

(33) Godat, E., Madalinski, G., Muller, L., Heilier, J.-F., Labarre, J., Junot, C., Enrique, C., and Lester, P. (2010) Chapter 2 - Mass Spectrometry-Based Methods for the Determination of Sulfur and Related Metabolite Concentrations in Cell Extracts. *Methods in Enzymology 473*, 41−76.

(34) Ageta, H., Asai, S., Sugiura, Y., Goto-Inoue, N., Zaima, N., and Setou, M. (2009) Layer-specific sulfatide localization in rat hippocampus middle molecular layer is revealed by nanoparticle-assisted

laser desorption/ionization imaging mass spectrometry. *Med. Mol. Morphol. 42*, 16−23.
(35) Cornett, D. S., Reyzer, M. L., Chaurand, P., and Caprioli, R. M. (2007) MALDI imaging mass spectrometry: molecular snapshots of biochemical systems. *Nat. Methods 4*, 828−833.
(36) Sjövall, P., Johansson, B., and Lausmaa, J. (2006) Localization of lipids in freeze-dried mouse brain sections by imaging TOF-SIMS. *Appl. Surf. Sci. 252*, 6966−6974.
(37) Van de Plas, R., De Moor, B., and Waelkens, E. (2007) Imaging mass spectrometry based exploration of biochemical tissue composition using peak intensity weighted PCA. *In Life Science Systems and Applications Workshop, 2007. LISA 2007. IEEE/NIH*; IEEE: Piscataway, NJ.
(38) George, G. N., Gorbaty, M. L., Kelemen, S. R., and Sansone, M. (1991) Direct determination and quantification of sulfur forms in coals from the Argonne Premium Sample Program. *Energy Fuels 5*, 93−97.
(39) Gnida, M., Yu Sneeden, E., Whitin, J. C., Prince, R. C., Pickering, I. J., Korbas, M. g., and George, G. N. (2007) Sulfur X-ray Absorption Spectroscopy of Living Mammalian Cells: An Enabling Tool for Sulfur Metabolomics. In Situ Observation of Uptake of Taurine into MDCK Cells. *Biochemistry 46*, 14735−14741.
(40) Pickering, I. J., Sneeden, E. Y., Prince, R. C., Block, E., Harris, H. H., Hirsch, G., and George, G. N. (2009) Localizing the Chemical Forms of Sulfur in Vivo Using X-ray Fluorescence Spectroscopic Imaging: Application to Onion (*Allium cepa*) Tissues. *Biochemistry 48*, 6846−6853.
(41) Pickering, I. J., Prince, R. C., Divers, T., and George, G. N. (1998) Sulfur K-edge X-ray absorption spectroscopy for determining the chemical speciation of sulfur in biological systems. *FEBS Lett. 441*, 11−14.
(42) Pickering, I. J., George, G. N., Yu, E. Y., Brune, D. C., Tuschak, C., Overmann, J., Beatty, J. T., and Prince, R. C. (2001) Analysis of Sulfur Biochemistry of Sulfur Bacteria using X-ray Absorption Spectroscopy. *Biochemistry 40*, 8138−8145.
(43) Rompel, A., Cinco, R. M., Latimer, M. J., McDermott, A. E., Guiles, R. D., Quintanilha, A., Sauer, K., Yachandra, V. K., and M.P, K. (1998) Sulfur K-edge X-ray absorption spectroscopy: A spectroscopic tool to examine the redox state of S-containing metabolites in vivo. *Proc. Natl. Acad. Sci. U.S.A. 95*, 6122−6127.
(44) Bohic, S., Murphy, K., Paulus, W., Cloetens, P., Salomeì, M., Susini, J., and Double, K. (2008) Intracellular Chemical Imaging of the Developmental Phases of Human Neuromelanin Using Synchrotron X-ray Microspectroscopy. *Anal. Chem. 80*, 9557−9566.
(45) Crippa, P., Eisner, M., Morante, S., Stellato, F., Vicentin, F., and Zecca, L. (2010) An XAS study of the sulfur environment in human neuromelanin and its synthetic analogs. *Eur. Biophys. J. 39*, 959−970.
(46) Jacob, C., Giles, G. I., Giles, N. M., and Sies, H. (2003) Sulfur and Selenium: The Role of Oxidation State in Protein Structure and Function. *Angew. Chem., Int. Ed. 42*, 4742−4758.
(47) Vogt, W. (1995) Oxidation of methionyl residues in proteins: Tools, targets, and reversal. *Free Radical Biol. Med. 18*, 93−105.
(48) Hackett, M. J., McQuillan, J. A., El-Assaad, F., Aitken, J. B., Levina, A., Cohen, D. D., Siegele, R., Carter, E. A., Grau, G. E., Hunt, N. H., and Lay, P. A. (2011) Chemical alterations to murine brain tissue induced by formalin fixation: implications for biospectroscopic imaging and mapping studies of disease pathogenesis. *Analyst 136*, 2941−2952.
(49) Madsen, S., Ottersen, O. P., and Storm-Mathisen, J. (1985) Immunocytochemical visualisation of taurine: neuronal localisation in the rat cerebellum. *Neurosci. Lett. 60*, 225−260.
(50) Guidotti, A., Badiani, G., and Pepeu, G. (1972) Taurine Distribution in Cat Brain. *J. Neurochem. 19*, 431−435.
(51) Palkovits, M., Elekes, I., Lang, T., and Patthy, A. (1986) Taurine levels in discrete brain nuclei of rats. *J. Neurochem. 47*, 1333−1335.
(52) Nadi, N. S., Mbride, W. J., and Aprison, M. H. (1977) Distribution of several amino acids in regions of the cerebellum of the rat1. *J. Neurochem. 28*, 453−455.
(53) Pirvola, U., and Panula, P. (1992) Distribution of taurine in the rat cerebellum and insect brain: application of a new antiserum against carbodiimide-conjugated taurine. *Histochem. J. 24*, 266−274.
(54) Ricci, G., Dupre, S., Federici, G., Spoto, G., Matarese, R. M., and Cavallini, D. (1978) Oxidation of hypotaurine to taurine by ultraviolet irradiation. *Physiol. Chem. Phys. 10*, 435−451.
(55) Oja, S. S., and Kontro, P. (1981) Oxidation of hypotaurine in vitro by mouse liver and brain tissues. *Biochim. Biophys. Acta, Gen. Subj. 677*, 350−357.
(56) Sekiyama, H., Kosugi, N., Kuroda, H., and Ohta, T. (1986) *Bull. Chem. Soc. Jpn. 59*, 575−579.
(57) George, M. J. (2000) XAS-Collect: A computer program for X-ray absorption spectroscopic data acquisition. *J. Synchrotron Radiat. 7*, 283−286.
(58) George, G. N. http://ssrl.slac..stanford.edu/exafspak.html.